



PERGAMON

Acta mater. Vol. 47, No. 5, pp. 1597–1611, 1999
© 1999 Published by Elsevier Science Ltd
On behalf of Acta Metallurgica Inc. All rights reserved
Printed in Great Britain
1359-6454/99 \$20.00 + 0.00

PII: S1359-6454(99)00020-8

CRYSTALLOGRAPHIC ASPECTS OF GEOMETRICALLY-NECESSARY AND STATISTICALLY-STORED DISLOCATION DENSITY

A. ARSENLIS and D. M. PARKS†

Department of Mechanical Engineering, Massachusetts Institute of Technology, Cambridge, MA 01239, U.S.A.

(Received 14 October 1998; accepted 22 December 1998)

Abstract—Classical plasticity has reached its limit in describing crystalline material behavior at the micron level and below. Its inability to predict size-dependent effects at this length scale has motivated the use of higher-order gradients to model material behavior at the micron level. The physical motivation behind the use of strain gradients has been based on the framework of geometrically-necessary dislocations (GNDs). A new but equivalent definition for Nye's dislocation tensor, a measure of GND density, is proposed, based on the integrated properties of dislocation lines within a volume. A discrete form of the definition is applied to redundant crystal systems, and methods for characterizing the dislocation tensor with realizable crystallographic dislocations are presented. From these methods and the new definition of the dislocation tensor, two types of three-dimensional dislocation structures are found: open periodic networks which have long-range geometric consequences, and closed three-dimensional dislocation structures which self-terminate, having no geometric consequence. The implications of these structures on the presence of GNDs in polycrystalline materials lead to the introduction of a Nye factor relating geometrically-necessary dislocation density to plastic strain gradients. © 1999 Published by Elsevier Science Ltd on behalf of Acta Metallurgica Inc. All rights reserved.

Keywords: Metals, Dislocations, theory, Mechanical properties, plastic

1. INTRODUCTION

Recent experiments have shown a size dependence in the mechanical behavior of materials at the sub-micron to micron level. Torsion of thin wires ranging in diameter from 12 to 170 μm has shown that there is increased torsional hardening as the diameter of the specimens decreases [1]. Bending of thin beams ranging in thickness from 12.5 to 50 μm has shown that there is increased material hardening in bending as the thickness of the beams decreases [2]. Micro-indentation experiments conducted at these length scales have shown similar phenomena. The measured indentation hardness of a crystal is found to increase as the depth of the indentation decreases from 10 to 1 μm [3,4]. All of these experiments have shown that the apparent material hardening increases as the size of the specimen decreases. Classical plasticity theory has been unable to account for the observed phenomena because it has no internal length scale in its formulation. All of the experiments which highlight these material size effects have associated with them large strain gradients with respect to the overall deformation. As a result, higher-order gradient theories have been proposed which incorporate a characteristic material

length scale [5,6] as a material property. The internal length scale has been introduced through dimensional arguments, based on the formulation of particular theories, and has been empirically inferred to be on the order of sub-microns to microns [1, 2, 6].

The strain gradient theories have been physically motivated by developments in dislocation mechanics. In particular, the framework of geometrically-necessary dislocations (GNDs) first introduced by Nye [7] and furthered by Ashby [8] and Kröner [9] has given a physical basis for strain-gradient-dependent material behavior. In descriptions of dislocations in crystals, dislocations could be separated into two different categories, geometrically-necessary dislocations which appeared in strain gradient fields due to geometrical constraints of the crystal lattice, and statistically-stored dislocations (SSDs) which evolved from random trapping processes during plastic deformation [8]. Although GNDs have provided the motivation for these theories, GNDs have been loosely interpreted, and continuum theories have mostly been concerned with finding relationships between the invariants of strain gradients and the mechanical behavior of materials [10,11].

The length scale dependence suggests that the underlying properties of the crystal lattice should

†To whom all correspondence should be addressed.

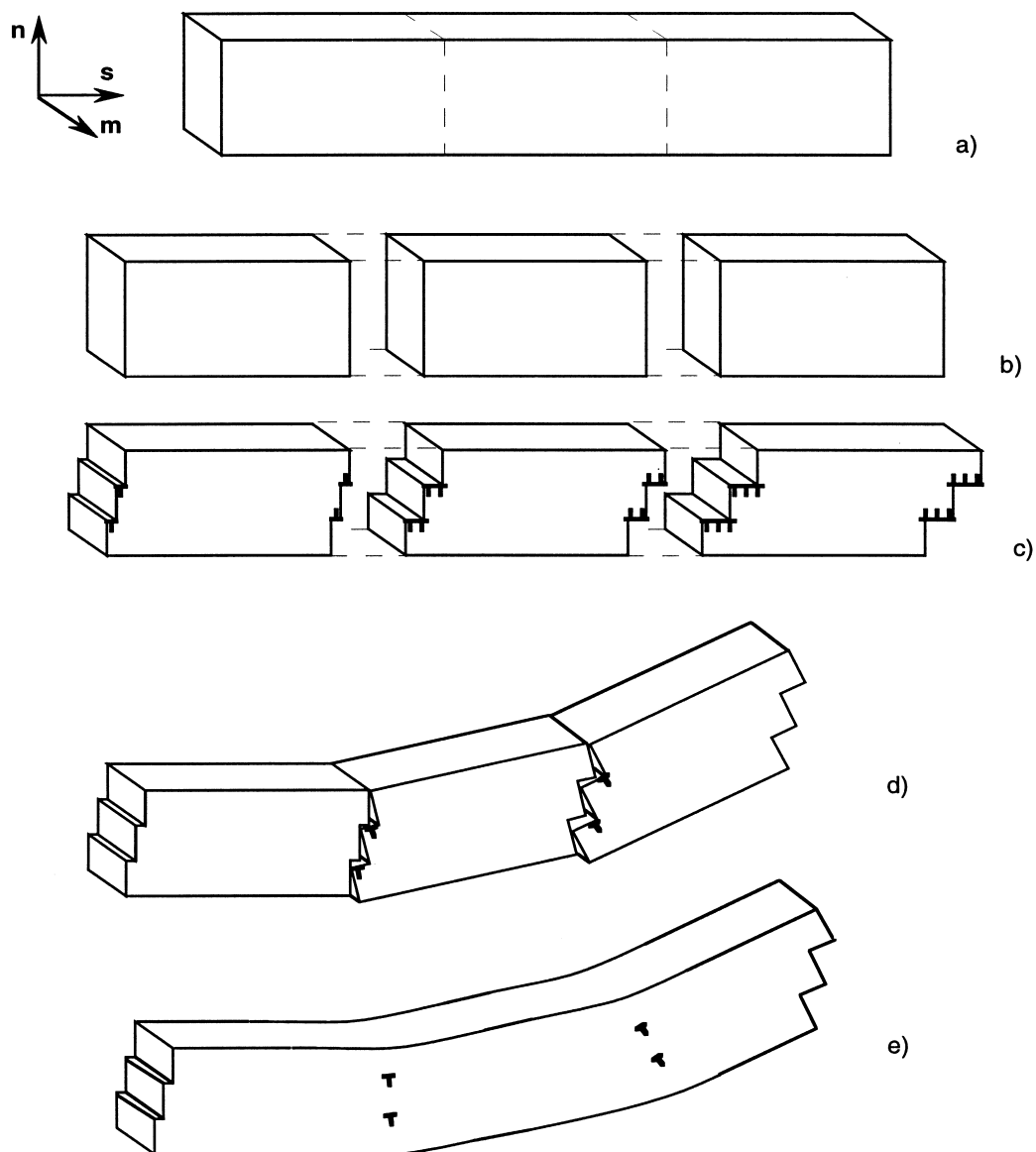


Fig. 1. Schematic process (a–e) through which geometrically-necessary edge dislocations accumulate.

play a larger role in the formulation of continuum strain gradient theories, and a more rigorous interpretation of GNDs, one which accounts for crystalline anisotropy, be implemented. As a first step in describing GND populations in a polycrystalline material, the properties of GNDs and SSDs in single crystals are investigated. This article discusses the physical arguments for the appearance of dislocations due to strain gradients and introduces a new definition for Nye's tensor, a quantity used to measure GND density, based on the integrated properties of dislocation lines within a volume. With this new definition, global properties of the two dislocation categories are immediately apparent. A discretized version of the integral relation is

developed to investigate the geometric properties of dislocations in crystals which can accommodate geometrical constraints with different dislocation arrangements. Two methods are introduced to calculate the GND density in these redundant crystals, and new SSD arrangements are discovered. The methods are applied to the face-centered cubic (f.c.c.) lattice to demonstrate the properties of the GNDs in this discrete formulation. The results of the single crystal investigation have important consequences on the presence of GNDs in polycrystalline materials, and a Nye factor is introduced which relates macroscopic strain gradients to scalar measures of GND density in polycrystalline materials.

2. CRYSTALLOGRAPHIC DISLOCATIONS FROM STRAIN GRADIENTS

Gradients in the plastic strain within crystalline materials give rise to dislocations in order to maintain continuity in the crystal. Furthermore, with knowledge of the crystalline orientation in relation to the strain gradient, the type of dislocation needed to maintain lattice continuity is also specified. The graphical arguments for the existence of these dislocations presented in this section are based on the two-dimensional constructs of Ashby [8] but have been extended to three-dimensions.

Consider the schematic in Fig. 1(a)–(e) of a simple crystal undergoing single slip on slip system “a”. The coordinate reference frame is set such that \mathbf{s}^a is a unit vector in the slip direction, \mathbf{n}^a the slip-plane unit normal, and $\mathbf{m}^a = \mathbf{s}^a \times \mathbf{n}^a$. Imagine that the material can be separated into three sections, and each section can be deformed independently of the others. Through expanding dislocation loops, the respective sections are plastically deformed such that the plastic strain increases linearly in the slip direction. When the dislocation loops reach the boundaries of each section, the screw portions

reach free boundaries and exit the material, but the edge portions of the loops encounter fictitious internal boundaries and remain as dipoles spread to either side of each section. The sections are then forced back together, and there are negative edge dislocations which do not annihilate, but remain in the material, leading to lattice curvature.

Mathematically, the relationship between the plastic strain gradient on a slip system and the edge dislocation density takes the following form:

$$\rho_{GN(e)}^a b = -\nabla \gamma^a \cdot \mathbf{s}^a = -\gamma_{,k}^a s_k^a \quad (1)$$

where $\rho_{GN(e)}^a$ is the geometrically-necessary positive edge dislocation density and b the magnitude of the Burgers vector on slip system a.

A similar construction can be created to illustrate the presence of screw dislocations due to strain gradients. The schematic in Fig. 2(a)–(e) shows the same single slip system material as in Fig. 1(a)–(e). In this figure, the material is again separated into three sections, and each section is deformed independently of the other. Through expanding dislocation loops, the sections are plastically deformed such that the plastic strain increases linearly in the

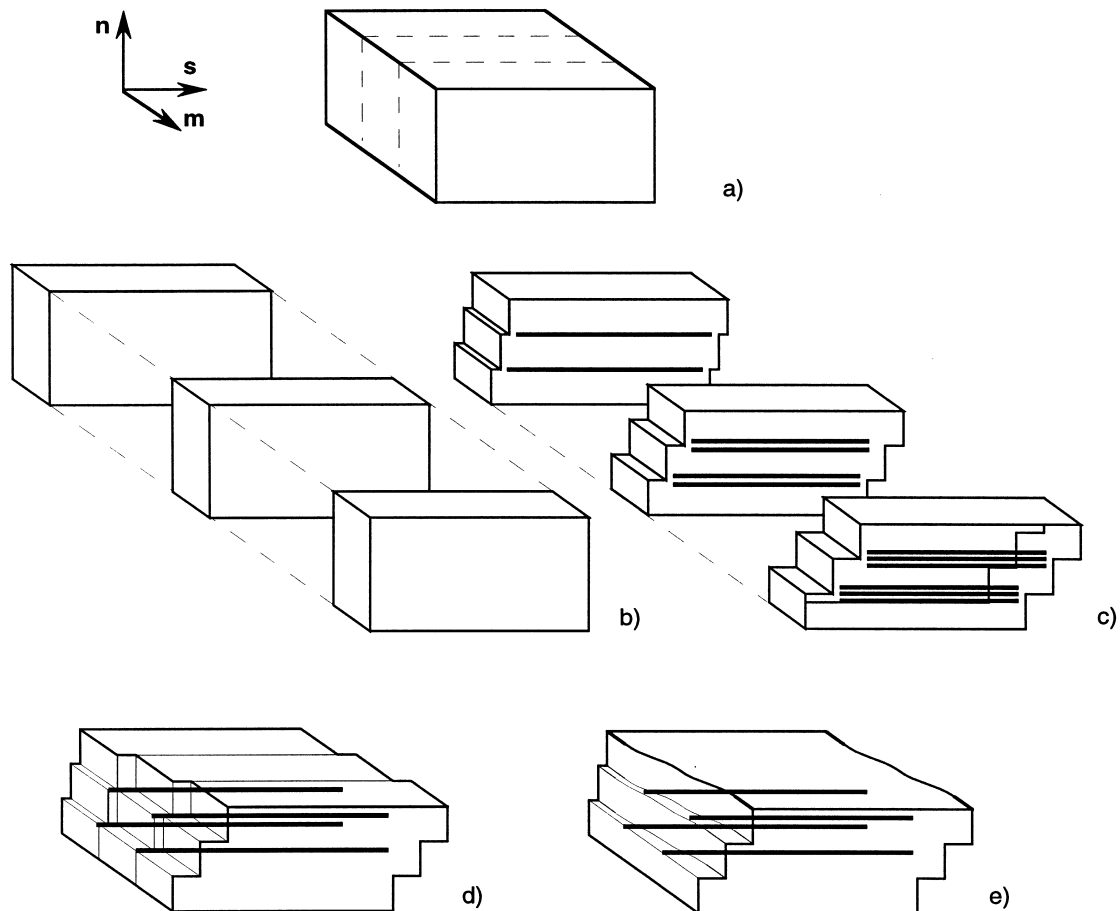


Fig. 2. Schematic process (a–e) through which geometrically-necessary screw dislocations accumulate.

\mathbf{m}^a -direction. When the dislocation loops reach the boundaries of each section, the edge portions reach free boundaries and exit the material, but the screw segments encounter fictitious internal boundaries and remain as dipoles spread to either side of each section. In the figure shown, the negative screw dislocations are illustrated, but there are also an equal number of positive screw dislocations, not shown, on the back (hidden) side of each section. When the sections are forced back together, there are positive screw dislocations which do not annihilate, remaining in the material and causing the lattice to warp.

The relationship between the plastic strain gradient on a slip system and the screw dislocation density takes the following form:

$$\rho_{GN(s)}^a b = \nabla \gamma^a \cdot \mathbf{m}^a = \gamma_{,k}^a m_k^a \quad (2)$$

where $\rho_{GN(s)}^a$ is the geometrically-necessary positive screw dislocation density and b the magnitude of the Burgers vector on slip system a .

These developments clearly show that gradients of plastic strain lead to the accumulation of dislocations. Furthermore, depending on the direction of the gradients in relation to the crystalline geometry, the type of dislocations needed to maintain lattice continuity can be specified, independent of the mechanism which caused the strain gradient. The plastic deformation in each example was accomplished through expanding dislocation loops, but the gradients of the plastic deformation were in different directions, leading to the accumulation of either geometrically-necessary edge or screw dislocations. The existence of the dislocations was necessary to maintain lattice continuity, and led to distortions of the the crystal lattice. Generally, the dislocation state associated with lattice distortion can be described in terms of a second-order tensor, to be discussed in the next section.

3. NYE'S TENSOR AND CONTINUOUSLY-DISTRIBUTED DISLOCATION DENSITY

In 1953, Nye introduced a dislocation tensor quantifying the state of dislocation of a lattice [7]. Nye's tensor, α_{ij} , is a representation of dislocations with Burgers vector i and line vector j . Considering continuously-distributed dislocations, Nye's tensor quantifies a special set of dislocations whose geometric properties are not canceled by other dislocations in the crystal. Consider the volume element shown in Fig. 3, which is a section of a crystal containing two edge dislocations threading through the volume. The most rigorous manner to describe the dislocation state in the volume would be to characterize the lines by two Dirac delta functions of strength b in space; however, such a quantification of dislocation density becomes overwhelming given the densities involved in plastic deformation processes ($\rho \doteq 10^{12}/\text{cm}^2$) [12]. Allowing such point densities to become continuously-distributed within a

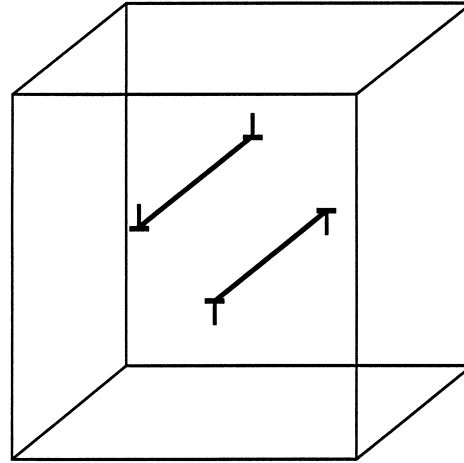


Fig. 3. An edge dislocation dipole in a volume element used to define Nye's tensor.

volume creates a more compact way of describing dislocations in space, but a result of this process is that some individual dislocation information is lost.

If the reference volume element over which dislocation properties will be continuously-distributed is taken to be the entire volume in Fig. 3, the net Nye's tensor of the element is zero because the dislocation density, as drawn, consists of two dislocations with common tangent line vector but opposite Burgers vector: these form a dislocation dipole. When the properties of each dislocation segment are distributed uniformly over the entire volume, the exact positions of the original dislocations are no longer relevant. In terms of Nye's tensor, an equivalent form would be to place the two dislocations on top of one another, allowing them to annihilate, leaving behind no dislocation density in the element. In any continuously-distributed dislocation formulation, individual dislocation dipoles, planar dislocation loops, and other three-dimensional self-terminating dislocation structures fully contained within the reference volume make no net contribution to Nye's tensor. The three-dimensional self-terminating dislocation structures mentioned here will be further developed in later sections. These redundant structures which make no contribution to Nye's tensor are considered statistically-stored dislocations (SSDs), and are believed to result from plastic deformation processes [8]. Once individual dislocation segments are considered to be uniformly distributed within a reference volume, Nye's tensor measures the non-redundant dislocation density within the volume. These non-redundant dislocations are believed to result from plastic strain gradient fields, as demonstrated in the previous section, and have geometric consequences on the crystal lattices. As a result, they are commonly referred to as geometrically necessary dislocations (GNDs).

Nye's tensor can easily be calculated for a volume element by a line integral over all dislocations within the volume. If \mathbf{b} is the Burgers vector of a dislocation with local unit tangent line direction \mathbf{t} , Nye's tensor, α_{ij} , can be defined as

$$\alpha_{ij} \equiv \frac{1}{V} \int_L b_i t_j ds \quad (3)$$

where V is the reference volume, ds an element of arc length along the dislocation line, and L the total length of dislocation line within V . Nye's tensor becomes a summation of the integrated properties of all the individual dislocation line segments in the volume. This integral relation also has the property of averaging the dislocation properties within the volume, thus converting clearly distinct dislocation lines into a uniformly distributed property within the volume. If each of the dislocation line segments is considered as a separate entity with constant Burgers vector, the definition of Nye's tensor can be rewritten as

$$\alpha_{ij} \equiv \frac{1}{V} \sum_{\xi} b_i^{\xi} \int_l t_j^{\xi} ds^{\xi} \quad (4)$$

where l is the length of a dislocation segment of type ξ . Inspection of this summation of integrals immediately shows global properties of Nye's tensor. Consider Fig. 4 of a dislocation threading through a reference volume element used to define Nye's tensor. If equation (4) is used to evaluate Nye's tensor for this element, the result becomes

$$\alpha_{ij} = \frac{1}{V} b_i (x_j^+ - x_j^-) \quad (5)$$

where \mathbf{x}^- and \mathbf{x}^+ are the positions of the starting and stopping points of the dislocation line segment, respectively. Equation (5) states that the only information from each dislocation line segment needed

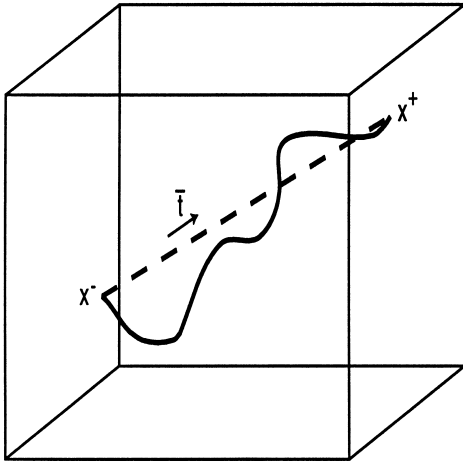


Fig. 4. A dislocation line threading through a reference volume element used to define Nye's tensor.

to calculate its contribution to Nye's tensor is its Burgers vector and two endpoints. The path that the dislocation line makes between these two points has no effect on the evaluation of Nye's tensor. Returning to Fig. 4, for the purpose of evaluating Nye's tensor, the curved dislocation line could be replaced by the dashed straight dislocation line having the same geometric properties. Equation (5) may be rewritten to reflect this substitution, with the result that it is the average tangent vector, $\bar{\mathbf{t}}$, and the secant length, \bar{l}^{ξ} , which are needed to calculate α_{ij} :

$$\alpha_{ij} = \frac{1}{V} \sum_{\xi} \bar{l}^{\xi} b_i^{\xi} \bar{t}_j^{\xi} \quad (6)$$

where

$$\bar{t}_j^{\xi} = \frac{(x_j^+ - x_j^-)}{\sqrt{(x_k^+ - x_k^-)(x_k^+ - x_k^-)}} \quad (7)$$

and

$$\bar{l}^{\xi} = \sqrt{(x_k^+ - x_k^-)(x_k^+ - x_k^-)} \quad (8)$$

Using the description of dislocation density as line length in a volume, the summation of geometric dislocation lengths, \bar{l}^{ξ} , in a reference volume, V , can be replaced by a summation of geometric dislocation density, ρ_{GN}^{ξ} , in the volume

$$\alpha_{ij} = \sum_{\xi} \rho_{GN}^{\xi} b_i^{\xi} \bar{t}_j^{\xi} \quad (9)$$

where

$$\rho_{GN}^{\xi} \equiv \frac{\bar{l}^{\xi}}{V} \quad (10)$$

Of course, the dislocation density described in equation (9) is not the total dislocation density of any arbitrary dislocation line segment, but it is the portion of the total dislocation density which has geometric consequences. The remaining density of the total line, which has no geometric consequence, must be considered statistical in character. For an arbitrary dislocation line segment, ξ , with a total density in a reference volume, V , defined by

$$\rho^{\xi} \equiv \frac{1}{V} \int_l ds^{\xi} \quad (11)$$

the portion of the total density which has no geometric consequence, and which would therefore be statistical in nature, would be

$$\rho_{SS}^{\xi} \equiv \rho^{\xi} - \rho_{GN}^{\xi} \quad (12)$$

where the subscript SS denotes that the dislocation density is considered statistically-stored. With this decomposition of total dislocation density, an arbitrary line threading through a reference volume element as in Fig. 4 may be separated into that portion of the total density which has geometric

effects, ρ_{GN} , and the portion of the total density which does not, ρ_{SS} .

Another result of the definition of Nye's tensor which becomes immediately apparent through equation (5) is that closed dislocation loops of constant Burgers vector have no net geometric consequence; i.e.

$$\alpha_{ij} = \frac{1}{V} b_i \oint t_j ds = 0_{ij}. \quad (13)$$

As a generalization of this property, any dislocation network structure which is topologically closed and is entirely contained within the reference volume also has no net contribution to Nye's tensor.

In this formulation of Nye's tensor, the size of the reference volume element over which the density is averaged plays a crucial role in defining the tensor. Consider again Fig. 3 of the dislocation dipole. If the reference volume elements were taken to be smaller than the entire volume shown, such that both dislocations did not populate the same element, Nye's tensor within each sub-volume would change, becoming non-zero. In the limit as the volume elements used to define the dislocation state become differential, Nye's tensor tends toward two delta functions that exactly describe the dislocation state. Selection of an appropriate reference volume element must take into account the scale of the geometric effects to be captured. A volume element that is too large with respect to the geometric constraints may miss the existence of important geometrically-derived dislocations in one portion of the element that, when averaged with other dislocations in the same element, create no net Nye's tensor. Conversely, a volume element which is too small may become too computationally intensive (too numerous) to manage, and may begin to reach length scales where dislocation density can no longer be considered continuously distributed, and discrete dislocation mechanics must be incorporated.

The definition of Nye's tensor proposed here is based on the description of dislocation density as line length in a reference volume. In Nye's original formulation of the dislocation tensor, dislocation density was described as a number density of lines piercing a plane. He defined the tensor in the following manner:

$$\alpha_{ij} = n b_i t_j \quad (14)$$

where n was the number density of dislocation lines with Burgers vector, \mathbf{b} , crossing a unit area normal to their unit tangent line vector, \mathbf{t} . This expression closely resembles the definition of the tensor in equation (9). In the procedure by which Nye described the dislocation tensor, the dislocations which constituted it were considered to be continuously distributed, and the tangent line vectors were implicitly constant. The discrete case, in which a material is segmented into volume elements, was

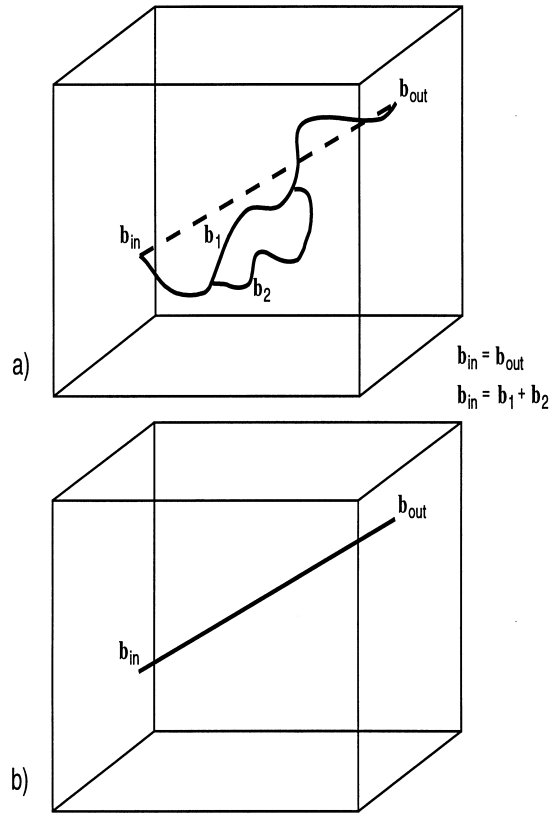


Fig. 5. A simple dislocation network with two junctions threading through a reference volume element used to define Nye's tensor (a), and its corresponding geometric fingerprint (b).

not considered in the original formulation. The expression proposed here is a generalization which can be applied to arbitrary dislocation arrangements, and the two definitions are equivalent because the dislocations which contribute to the geometric density in the bulk must pierce the surface that encloses the reference volume, as a consequence of equation (13). Consider Fig. 5(a) which represents a relatively simple dislocation arrangement containing two dislocation junctions threading through the volume. By applying equation (3) to the system, it can be shown that a geometrically equivalent dislocation arrangement would be a single straight dislocation segment as shown in Fig. 5(b). This results from the property that Burgers vector is conserved through line segments and their junctions. Applying both equations (3) and (4) to the simplified structure in Fig. 5(b) yields the same value for Nye's tensor. The definitions are equivalent because of the stereological relationship between the two descriptions of dislocation density.

4. LATTICE-GEOMETRIC CONSEQUENCES OF NYE'S TENSOR

Plastic strain gradients necessarily lead to the existence of dislocations in crystalline materials to

maintain lattice continuity. Nye's tensor provides a measure of these geometrically-derived dislocations, and a non-zero Nye's tensor leads to lattice curvature, neglecting elastic strain gradients in the material. Introduction of dislocations of the same type into a crystal causes the lattice to curve and generally warp, and a tensor quantifying such lattice curvature must be closely related to Nye's tensor. The curvature tensor, κ_{ij} , is defined as a small right handed lattice rotation of magnitude $\delta\vartheta$ about the i -axis for a unit change of position of magnitude δx in the j -direction:

$$\delta\vartheta_i = \kappa_{ij}\delta x_j. \quad (15)$$

Nye's tensor relates the GND density to lattice curvature in the following manner:

$$\kappa_{ij} = -\alpha_{ji} + \frac{1}{2}\delta_{ji}\alpha_{kk} \quad (16)$$

which is the same result that Nye derived but with a different sign convention [7]. There is also a contribution from elastic strain gradients to the total lattice curvature. A complete and rigorous derivation of the relationship between strain gradients, curvature, and the new definition of Nye's tensor is presented in this section.

The following derivation closely mirrors a previous analysis by Fleck and Hutchinson [10]. The displacement gradient, $u_{i,j}$, can be additively decomposed into the plastic slip tensor, γ_{ij} , the skew lattice rotation tensor, ϕ_{ij} , and the symmetric elastic strain tensor, $\epsilon_{ij}^{\text{el}}$, as shown in equation (17):

$$u_{i,k} = \gamma_{ik} + \phi_{ik} + \epsilon_{ik}^{\text{el}}. \quad (17)$$

The curl of the displacement gradient vanishes because of the symmetry of the second gradient; this also implies that deformation occurs in such a way that the body remains simply connected. Such a procedure, when performed on equation (17), produces

$$e_{pjk}u_{i,kj} = e_{pjk}\gamma_{ik,j} + e_{pjk}\phi_{ik,j} + e_{pjk}\epsilon_{ik,j}^{\text{el}} = 0_{pi} \quad (18)$$

where e_{pjk} are the cartesian components of the alternating tensor. The components of the lattice rotation tensor, ϕ_{ik} , can be written in terms of the lattice rotation vector, ϑ_b , according to

$$\phi_{ik} = e_{ilk}\vartheta_l. \quad (19)$$

Substitution of equation (19) into equation (18) gives

$$e_{pjk}\gamma_{ik,j} + e_{pjk}e_{ilk}\vartheta_{l,j} + e_{pjk}\epsilon_{ik,j}^{\text{el}} = 0_{pi}. \quad (20)$$

Using the definition of $\kappa_{ij} = \vartheta_{l,j}$ implied by equation (15), inversion of equation (20) gives

$$\kappa_{pi} = e_{pjk}\gamma_{ik,j} - \frac{1}{2}\delta_{pi}e_{sjk}\gamma_{sk,j} + e_{pjk}\epsilon_{ik,j}^{\text{el}}. \quad (21)$$

Since plastic deformation is a result of the slip on crystallographic planes, γ_{ij} can be written as a sum

of crystallographic shears such that

$$\gamma_{ik} = \sum_a \gamma^a s_i^a n_k^a \quad (22)$$

where \mathbf{s}^a is the slip direction and \mathbf{n}^a the slip-plane normal direction of slip system a on which a plastic shear, γ^a , has occurred. Applying the curl operation inside the summation yields

$$e_{pjk}\gamma_{ik,j} = \sum_a e_{pjk}\gamma_j^a s_i^a n_k^a = \sum_a \gamma_j^a s_i^a (s_j^a m_p^a - m_j^a s_p^a) \quad (23)$$

where the last step follows from the definition $\mathbf{m}^a = \mathbf{s}^a \times \mathbf{n}^a$. Using equations (1) and (2), the right side of equation (23) can be replaced by dislocation densities:

$$e_{pjk}\gamma_{ik,j} = \sum_a -\rho_{GN(e)}^a b^a s_i^a m_p^a - \rho_{GN(s)}^a b^a s_i^a s_p^a. \quad (24)$$

Dislocation densities are considered to be defined as length of line in a reference volume, which allows for a substitution of variables in equation (24), leading to

$$e_{pjk}\gamma_{ik,j} = -\sum_a \rho_{GN}^a b^a s_i^a \bar{t}_p^a \quad (25)$$

where

$$\rho_{GN}^a \equiv \sqrt{(\rho_{GN(e)}^a)^2 + (\rho_{GN(s)}^a)^2} \quad (26)$$

and

$$\bar{t}_p^a \equiv \frac{\rho_{GN(e)}^a m_p^a + \rho_{GN(s)}^a s_p^a}{\rho_{GN}^a}. \quad (27)$$

The right-hand side of equation (25) is the expression used to define Nye's tensor in equation (9) relating the gradient of plastic slip to Nye's tensor. Substitution of equation (25) into equation (21) using the definition of Nye's tensor in equation (9) yields

$$\kappa_{pi} = -\alpha_{ip} + \frac{1}{2}\delta_{pi}\alpha_{kk} + e_{pjk}\epsilon_{ik,j}^{\text{el}} \quad (28)$$

which is the same expression as equation (16) in the absence of elastic strain gradients.

The relationships among plastic slip gradients, geometrically-necessary dislocation density, Nye's tensor, and lattice curvature presented thus far are general and apply to any crystal lattice. In the next section, the presence of GNDs in crystals with a high degree of symmetry is considered. The symmetry allows for multiple dislocation configurations to have the same total geometric properties. Therefore, the crystallographic dislocation state resultant from the geometric constraints is indeterminate. The indeterminacy can be resolved using two methods, as proposed in the next section.

5. UNIQUE DESCRIPTION OF GNDs IN REDUNDANT CRYSTALS

The most rigorous manner to describe crystallographic dislocation density would be to develop initial conditions and evolution laws for their densities and their interactions. The geometrical properties of such dislocation distributions would just be a consequence of the evolving state. Nye's tensor would be a simple result of the density at any instant, and plastic strain would result from the motion of density through the volume. Such evolution laws on a field basis have not been developed as of yet, but the plastic slip gradient field imposes geometric constraints on the dislocation density state which disallow many crystallographic dislocation distributions.

In crystals with a high degree of symmetry, the geometric constraints can be satisfied with many different dislocation configurations due to their redundancy, much the same as a given plastic deformation can be performed by different combinations of slip on individual systems. In such redundant crystals, the number of distinct dislocation "types", each with its own geometric properties, exceeds the nine independent values in Nye's tensor, but the concept of geometrically-necessary dislocations implies a minimization of density. Consider again Fig. 4 of the dislocation threading through a reference volume. It was shown that its total dislocation density could be decomposed into a geometrically-necessary part and a statistically-stored part. The geometrically-necessary part was the minimum dislocation density needed to span the two endpoints of the dislocation line segment. If the only information from which crystallographic dislocation densities are to be determined is the result from geometric constraints, then the crystallographic dislocation density derived from the constraints must be a minimum density. Anything above the geometric minimum necessary would (necessarily!) incorporate some statistical character which cannot be determined through geometric arguments. By considering different density normalizations and minimizing the dislocation density with respect to those normalizations, a unique description of crystallographic GNDs can be found.

The first step in finding the GND configuration on a crystallographic basis is to discretize the dislocation space of a crystal. The Burgers vectors in a crystal are already discrete, but the tangent line vector of a dislocation is free to occupy any direction on the slip plane (if dislocations are allowed to climb, even this restrictive condition no longer holds!). The tangent line vectors must be discretized in such a fashion that the discretized space is well representative of the actual dislocation space. The discretized Burgers vector, \mathbf{b} , and tangent line vectors, \mathbf{t} , form n -pairs of geometric dislocation properties. Nye's tensor, $\boldsymbol{\alpha}$, can be written as a

summation of dislocation dyadics, \mathbf{d}_i , premultiplied by a scalar dislocation density, ρ_i , as follows:

$$\boldsymbol{\alpha} = \sum_{i=1}^n \rho_i \mathbf{d}_i \quad (29)$$

where the dislocation dyadic is given by

$$\mathbf{d}_i = \mathbf{b}^i \otimes \mathbf{t}^i. \quad (30)$$

Equation (29) can be rewritten such that Nye's tensor, represented as a nine-dimensional column vector Λ containing the components of $\boldsymbol{\alpha}$, is the result of a linear operator, \mathbf{A} , acting on the n -dimensional crystallographic dislocation density vector, ρ , as

$$\mathbf{A}\rho = \Lambda. \quad (31)$$

The null space of operator \mathbf{A} yields those combinations of crystallographic dislocation density which have no geometric consequence; thus these combinations can be considered as statistically-stored. Such dislocation density groups are placed in a subspace of the n -dimensional ρ -space, ρ_{SS} ; the dimension of the statistically-stored dislocation density subspace is $n - 9$.

In considering GNDs, there are two minimizations which can be considered. One minimization, L^2 , is geometrically motivated through equation (26) and minimizes the sum of the squares of the resulting dislocation densities. The discretization of the dislocation space only allows certain dislocations on the slip plane to exist, and the L^2 minimization takes this into account by being able to combine dislocation line lengths into a single dislocation line length which may not exist within the original discretization. The other minimizing technique, L^1 , is energetically motivated. By considering dislocation density as line length through a volume, the total dislocation line energy can be minimized by finding the dislocation configuration with the smallest total line length.

Mathematically, the L^2 minimization is the easier of the two methods to compute. The functional, $C(\rho, y)$, to be minimized takes the form

$$C(\rho, y) = \rho^T \rho + y^T (\mathbf{A}\rho - \Lambda) \quad (32)$$

where the nine-dimensional vector y contains the Lagrange multipliers. The solution can be found explicitly because it follows from singular value decomposition, having the following mathematical form:

$$\rho_{GN} = (\mathbf{A}^T \mathbf{A})^{-1} \mathbf{A}^T \Lambda \equiv \mathbf{B}\Lambda \quad (33)$$

which gives an explicit formula for the crystallographic GND density, ρ_{GN} , for any given value of Nye's tensor. Furthermore, ρ_{GN} calculated in this manner describes a dislocation density subspace which is orthogonal to ρ_{SS} such that $(\rho_{GN})^T \rho_{SS} = 0$, and the two subspaces span the total n -dimensional space of crystallographic dislocation densities.

There is no explicit formula for determining ρ_{GN} from Nye's tensor with respect to the L^1 minimum. Using this technique, the functional, $D(\rho, y)$, to be minimized takes the form

$$D(\rho, y) = \sum_{i=1}^n |\rho_i| + y^T(\mathbf{A}\rho - \Lambda) \quad (34)$$

where the nine-dimensional vector y contains the Lagrange multipliers. A linear simplex method is implemented to calculate ρ_{GN} for each different value of Nye's tensor. The resultant crystallographic dislocation density vector does not lie outside the ρ_{SS} subspace like the one obtained using the L^2 minimization. The two techniques are demonstrated on a face-centered cubic (f.c.c.) crystal in the following sections to illustrate the properties of each normalization, and the null space of \mathbf{A} is also analyzed to determine the properties of ρ_{SS} in redundant crystals.

6. GEOMETRICALLY-NECESSARY DISLOCATIONS IN F.C.C. CRYSTALS

Face-centered cubic crystals have slip systems in which the slip planes are of $\{111\}$ type and the slip directions are of $\langle 110 \rangle$ type. Although any discrete basis of dislocations which exist in the crystal may be considered, a natural choice is to limit the dislocations to only pure edge and pure screw types as Kubin *et al.* have done in their dislocation simulations [13]. Adopting this discretization, there are a total of 18 different dislocation types: 12 edge and six screw dislocations. The dislocations and their line properties are given in Table 1. Crystallographic dislocation density is described by an 18-dimensional vector in which each distinct dislocation type receives its own index, and ρ_i is the density of the i th dislocation type. Nye's tensor has only nine independent components; therefore, when describing the dislocation state in terms of crystallo-

graphic dislocation densities, the problem is under-defined, much like the indeterminacy of apportioning slip on crystallographic planes based on a known plastic deformation.

The geometric properties of the crystallographic dislocation densities were mapped onto the f.c.c. unit cell using equation (9), and the indices of Nye's tensor became the three orthonormal directions of the f.c.c. unit cell. A set of nine vectors were found which led to no contribution in Nye's tensor. These null vectors can be considered as the redundant or SSDs and will be discussed in detail in the next section. The GND density was calculated using the two different techniques outlined in the previous section, and the resultant GND distributions from the L^2 and L^1 minimizations will be presented independently and compared at the end of this section.

Using the singular value decomposition described above, a set of nine crystallographic dislocation vectors were obtained which minimized the sum of the squares of the densities and satisfied the geometric requirements of Nye's tensor. Table 2 shows the matrix which can be used to compute a general crystallographic dislocation distribution from GND density using L^2 minimization and the SSD density with $\langle 100 \rangle$ directions as the basis vectors of Nye's tensor. The first nine columns of this matrix make up the matrix, \mathbf{B} , in equation (33). Note that there are negative crystallographic dislocation densities in the GND vectors. The negative densities appear as a result of the discrete dislocation basis chosen. The basis defines the right-handed edge and screw dislocations as being positive densities, and left-handed edge and screw dislocation densities are considered negative. The L^1 formulation employs an expanded basis, and the necessity to interpret negative densities is eliminated.

Upon inspection of the nine GND vectors, there are only two distinct dislocation arrangements which are formed: one which exhibits the same properties as a $\langle 100 \rangle \langle 100 \rangle$ screw dislocation, and one which exhibits the same properties as a $\langle 100 \rangle \times \langle 010 \rangle$ edge dislocation on the f.c.c. unit cell. The other seven density vectors are just orthogonal transformations of these two GND vectors. In f.c.c. materials, dislocations of $\langle 100 \rangle$ type are not preferred, but an arrangement of crystallographic dislocations can be formed which has the same geometric properties as a $\langle 100 \rangle$ type dislocation. This arrangement for a screw dislocation is mathematically described by the first density vector (column 1) in Table 2, and is graphically presented in Fig. 6 by interpreting the densities as line lengths within a volume described by equation (9). Figure 6 shows the resulting double-helical structure, with screw dislocations around the perimeter of the structure and a mix of edge and screw dislocations in the center. The global geometric properties of this dislocation structure are the same as those of a

Table 1. The dislocation basis used to describe the dislocation state in f.c.c. crystals

Density	t	s	n
ρ_1	$\frac{1}{\sqrt{6}}[\bar{1}\bar{1}2]$	$\frac{1}{\sqrt{2}}[\bar{1}10]$	$\frac{1}{\sqrt{3}}[111]$
ρ_2	$\frac{1}{\sqrt{6}}[\bar{1}2\bar{1}]$	$\frac{1}{\sqrt{2}}[10\bar{1}]$	$\frac{1}{\sqrt{3}}[11\bar{1}]$
ρ_3	$\frac{1}{\sqrt{6}}[2\bar{1}\bar{1}]$	$\frac{1}{\sqrt{2}}[0\bar{1}1]$	$\frac{1}{\sqrt{3}}[\bar{1}11]$
ρ_4	$\frac{1}{\sqrt{6}}[\bar{1}\bar{1}2]$	$\frac{1}{\sqrt{2}}[\bar{1}\bar{1}0]$	$\frac{1}{\sqrt{3}}[\bar{1}\bar{1}\bar{1}]$
ρ_5	$\frac{1}{\sqrt{6}}[\bar{1}2\bar{1}]$	$\frac{1}{\sqrt{2}}[101]$	$\frac{1}{\sqrt{3}}[1\bar{1}\bar{1}]$
ρ_6	$\frac{1}{\sqrt{6}}[2\bar{1}\bar{1}]$	$\frac{1}{\sqrt{2}}[01\bar{1}]$	$\frac{1}{\sqrt{3}}[\bar{1}\bar{1}\bar{1}]$
ρ_7	$\frac{1}{\sqrt{6}}[\bar{1}\bar{1}2]$	$\frac{1}{\sqrt{2}}[\bar{1}10]$	$\frac{1}{\sqrt{3}}[\bar{1}\bar{1}1]$
ρ_8	$\frac{1}{\sqrt{6}}[\bar{1}2\bar{1}]$	$\frac{1}{\sqrt{2}}[\bar{1}01]$	$\frac{1}{\sqrt{3}}[\bar{1}\bar{1}\bar{1}]$
ρ_9	$\frac{1}{\sqrt{6}}[2\bar{1}\bar{1}]$	$\frac{1}{\sqrt{2}}[0\bar{1}1]$	$\frac{1}{\sqrt{3}}[\bar{1}\bar{1}\bar{1}]$
ρ_{10}	$\frac{1}{\sqrt{6}}[\bar{1}\bar{1}2]$	$\frac{1}{\sqrt{2}}[\bar{1}\bar{1}0]$	$\frac{1}{\sqrt{3}}[\bar{1}\bar{1}\bar{1}]$
ρ_{11}	$\frac{1}{\sqrt{6}}[\bar{1}2\bar{1}]$	$\frac{1}{\sqrt{2}}[\bar{1}0\bar{1}]$	$\frac{1}{\sqrt{3}}[\bar{1}\bar{1}\bar{1}]$
ρ_{12}	$\frac{1}{\sqrt{6}}[2\bar{1}\bar{1}]$	$\frac{1}{\sqrt{2}}[0\bar{1}1]$	$\frac{1}{\sqrt{3}}[\bar{1}\bar{1}\bar{1}]$
ρ_{13}	$\frac{1}{\sqrt{2}}[110]$	$\frac{1}{\sqrt{2}}[110]$	$\frac{1}{\sqrt{3}}[\bar{1}\bar{1}\bar{1}]$ or $\frac{1}{\sqrt{3}}[\bar{1}\bar{1}\bar{1}]$
ρ_{14}	$\frac{1}{\sqrt{2}}[101]$	$\frac{1}{\sqrt{2}}[101]$	$\frac{1}{\sqrt{3}}[\bar{1}\bar{1}\bar{1}]$ or $\frac{1}{\sqrt{3}}[\bar{1}\bar{1}\bar{1}]$
ρ_{15}	$\frac{1}{\sqrt{2}}[011]$	$\frac{1}{\sqrt{2}}[011]$	$\frac{1}{\sqrt{3}}[\bar{1}\bar{1}\bar{1}]$ or $\frac{1}{\sqrt{3}}[\bar{1}\bar{1}\bar{1}]$
ρ_{16}	$\frac{1}{\sqrt{2}}[\bar{1}10]$	$\frac{1}{\sqrt{2}}[\bar{1}10]$	$\frac{1}{\sqrt{3}}[111]$ or $\frac{1}{\sqrt{3}}[\bar{1}\bar{1}\bar{1}]$
ρ_{17}	$\frac{1}{\sqrt{2}}[10\bar{1}]$	$\frac{1}{\sqrt{2}}[10\bar{1}]$	$\frac{1}{\sqrt{3}}[111]$ or $\frac{1}{\sqrt{3}}[\bar{1}\bar{1}\bar{1}]$
ρ_{18}	$\frac{1}{\sqrt{2}}[0\bar{1}1]$	$\frac{1}{\sqrt{2}}[0\bar{1}1]$	$\frac{1}{\sqrt{3}}[111]$ or $\frac{1}{\sqrt{3}}[\bar{1}\bar{1}\bar{1}]$

Table 2. The linear operator used to create geometrically allowed dislocation density from Nye's tensor and statistically stored dislocation density. The first nine columns form the matrix **B** in equation (33) weighted by the components of Nye's tensor with (100) basis vectors. The last nine columns represent non-dipole components of the statistically-stored dislocation density, weighted by the parameters λ_i independent of Nye's tensor

ρ_1	a	$7c$	$-13c$	$-7c$	$-a$	$13c$	c	$-c$	0	3	1	1	0	0	0	0	0	0	α_{11}
ρ_2	$-a$	$13c$	$-7c$	$-c$	0	c	$7c$	$-13c$	a	0	-2	1	0	0	0	0	0	0	α_{12}
ρ_3	0	c	$-c$	$-13c$	a	$7c$	$13c$	$-7c$	$-a$	0	1	-2	0	0	0	0	0	0	α_{13}
ρ_4	a	$-7c$	$13c$	$7c$	$-a$	$13c$	$-c$	$-c$	0	0	0	0	1	1	0	0	0	0	α_{21}
ρ_5	$-a$	$-13c$	$7c$	c	0	c	$-7c$	$-13c$	a	3	0	0	-2	1	0	0	0	0	α_{22}
ρ_6	0	$-c$	c	$13c$	a	$7c$	$-13c$	$-7c$	$-a$	0	0	0	1	-2	0	0	0	0	α_{23}
ρ_7	a	$-7c$	$-13c$	$7c$	$-a$	$-13c$	c	c	0	0	0	0	0	0	1	1	0	0	α_{31}
ρ_8	$-a$	$-13c$	$-7c$	c	0	$-c$	$7c$	$13c$	a	0	0	0	0	0	-2	1	0	0	α_{32}
ρ_9	0	$-c$	$-c$	$13c$	a	$-7c$	$13c$	$7c$	$-a$	3	0	0	0	0	1	-2	0	0	α_{33}
ρ_{10}	a	$7c$	$13c$	$-7c$	$-a$	$-13c$	$-c$	c	0	1	0	0	0	0	0	0	1	1	λ_1
ρ_{11}	$-a$	$13c$	$7c$	$-c$	0	$-c$	$-7c$	$13c$	$-a$	1	0	0	0	0	0	0	-2	1	λ_2
ρ_{12}	0	c	c	$-13c$	a	$-7c$	$-13c$	$7c$	$-a$	1	0	0	0	0	0	0	1	-2	λ_3
ρ_{13}	$5d$	e	0	e	$5d$	0	0	0	$-d$	0	0	0	$-\sqrt{3}$	$\sqrt{3}$	$-\sqrt{3}$	$\sqrt{3}$	0	0	λ_4
ρ_{14}	$5d$	0	e	0	$-d$	0	e	0	$5d$	0	0	0	0	$-\sqrt{3}$	0	0	0	$-\sqrt{3}$	λ_5
ρ_{15}	$-d$	0	0	0	$5d$	e	0	e	$5d$	0	0	0	0	0	$\sqrt{3}$	0	$\sqrt{3}$	0	λ_6
ρ_{16}	$5d$	$-e$	0	$-e$	$5d$	0	0	0	$-d$	0	$-\sqrt{3}$	$\sqrt{3}$	0	0	0	0	$-\sqrt{3}$	$\sqrt{3}$	λ_7
ρ_{17}	$5d$	0	$-e$	0	$-d$	0	$-e$	0	$5d$	0	0	$-\sqrt{3}$	0	0	0	$-\sqrt{3}$	0	0	λ_8
ρ_{18}	$-d$	0	0	0	$5d$	$-e$	0	$-e$	$5d$	0	$\sqrt{3}$	0	0	$\sqrt{3}$	0	0	0	0	λ_9

where $a = \frac{\sqrt{3}}{9}$ $c = \frac{\sqrt{3}}{84}$ $d = \frac{1}{18}$ $e = \frac{3}{14}$

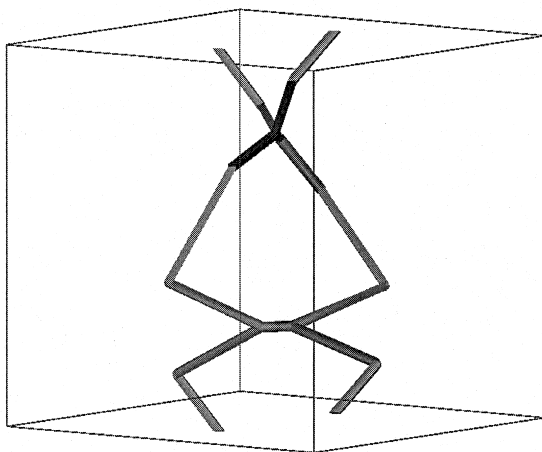
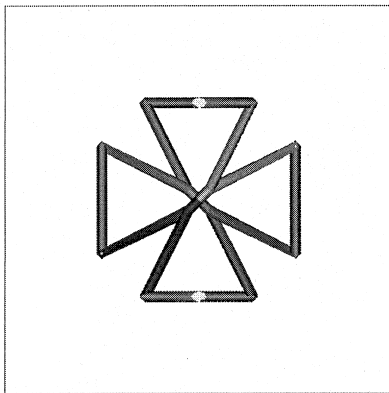


Fig. 6. A periodic dislocation network derived through the L^2 minimization scheme which has the same geometric properties as a $\langle 100 \rangle \langle 100 \rangle$ positive screw dislocation.

[100] type screw dislocation. It is periodic in the direction of the dislocation line vector, [100], and there is a discrete rotational symmetry about the [100] axis, much as a [100][100] screw dislocation would have if it existed in f.c.c. crystals.

A similar arrangement can be created to describe a $\langle 100 \rangle \langle 010 \rangle$ edge dislocation in f.c.c. materials. This arrangement is mathematically described by the second vector (column 2) in Table 2, and is graphically shown in Fig. 7. It is made up of 12 edge dislocations, and two screw dislocations which cross at the center of the structure. The structure is again periodic in the line direction, and it has the same global geometric properties as the $\langle 100 \rangle \langle 010 \rangle$ edge dislocation. The structure also has a mirror symmetry on either side of the virtual extra atomic half plane. With these nine vectors, a dislocation with arbitrary Burgers vector and line direction can be described as a periodic structure made up of the 18 crystallographic dislocation densities in f.c.c. materials.

To implement the L^1 minimization of GNDs using the linear simplex method, the discretization employed for the L^2 minimization had to be altered such that only positive densities were considered. This was accomplished by giving the left-handed screw and edge dislocations their own index, i , and requiring all densities to be positive. The size of the discrete dislocation basis doubled, introducing 18 more SSD vectors. The new SSD vectors introduced through this discretization represent dislocation dipoles formed by right- and left-handed dislocations of equal length. Dislocation dipoles are what are classically thought to result from plastic deformation, and are the most common example of SSDs, and although they were not accounted for in

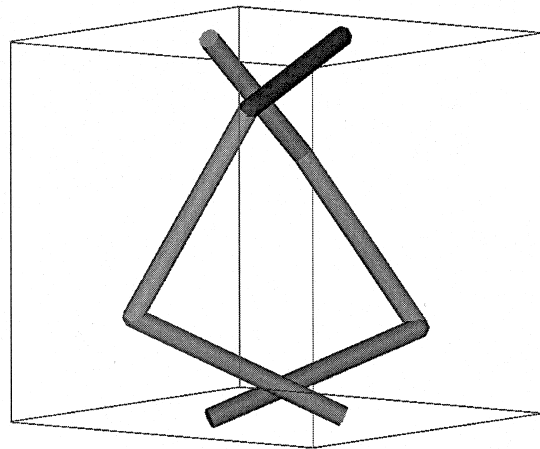
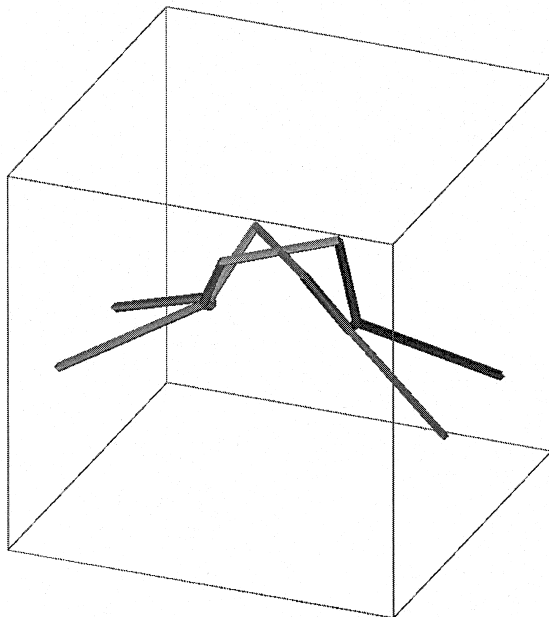
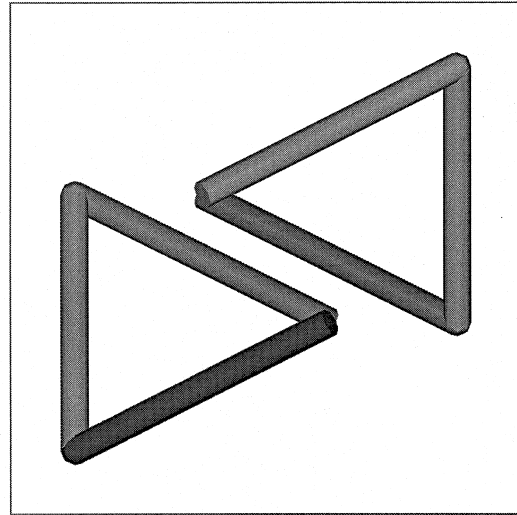
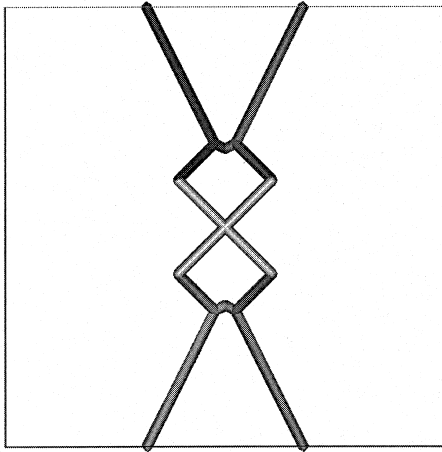


Fig. 7. A periodic dislocation network derived through the L^2 minimization scheme which has the same geometric properties as a $\langle 100 \rangle \langle 010 \rangle$ positive edge dislocation.

Fig. 8. A periodic dislocation network derived through the L^1 minimization scheme which has the same geometric properties as a $\langle 100 \rangle \langle 100 \rangle$ positive screw dislocation.

the discretized space employed in the L^2 formulation, they do appear in this expanded space.

To calculate the GND density using the linear simplex method, a feasible solution was found through row reduction of the matrix \mathbf{A} from equation (31) and back substitution. The minimal L^1 density was found through an iterative process, and had to be conducted for each different value of Nye's tensor. In order to compare the results of L^1 and L^2 minimizations, the dislocation structures for the $\langle 100 \rangle \langle 100 \rangle$ screw dislocations and the $\langle 100 \rangle \langle 010 \rangle$ edge dislocations were also found using the L^1 minimization technique. The crystallographic dislocation structure for a $[100][100]$ screw dislocation using the L^1 minimization technique is depicted in Fig. 8. The

structure consists of two separate dislocation lines with Burgers vectors $[110]$ and $[1\bar{1}0]$, respectively, and the same average tangent line vector $[100]$, and each threading dislocation line consists of three dislocation line segments. The crystallographic dislocation structure for the L^1 minimal $[100][010]$ edge dislocation found is shown in Fig. 9. It also is made up of two separate dislocation lines with Burgers vectors $[110]$ and $[1\bar{1}0]$, respectively, and the same average tangent line vector $[010]$, and each threading dislocation line consists of two dislocation line segments.

The purpose of this exercise in crystallographic GNDs was to find a method to best represent the actual GND dislocation arrangements in crystals. Both of the methods found periodic dislocation arrangements which threaded through the reference volume and had the same global geometric effects. Comparing the screw and edge dislocation arrangements obtained with the two different techniques,

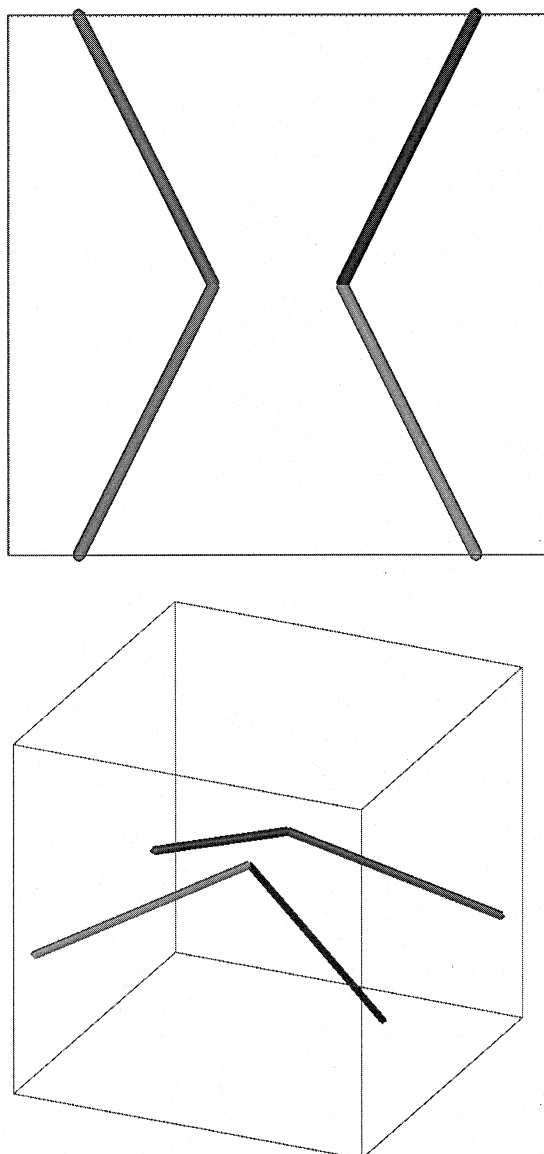


Fig. 9. A periodic dislocation network derived through the L^1 minimization scheme which has the same geometric properties as a $\langle 100 \rangle (010)$ positive edge dislocation.

the L^1 minimization appears to be a more promising technique than the L^2 technique for determining GNDs. In each case, the L^1 method created dislocation structures which were composed of two separate dislocation lines with constant Burgers vectors threading through the volume; the arrangements created by the L^2 method were much more complicated in the sense that they contained more dislocation segments in their structures and also required the formation of intricate junctions. The total dislocation line length needed to describe the $[100][010]$ edge dislocation with the L^2 minimization was a factor of 1.25 greater than the corresponding L^1 minimization. The total line length needed to describe the $[100][100]$ screw dislocation with the L^2 minimization was a factor of 1.01 greater than the

L^1 minimization. Note that this particular crystalline orientation required the longest total dislocation line length to represent a geometrically-necessary screw dislocation calculated using the L^1 minimization. All other crystalline orientations required shorter total dislocation line lengths. The disadvantage of employing the L^1 method over the L^2 method is that there is no explicit formulation using the linear simplex method to determine ρ_{GN} from Nye's tensor, whereas the singular value decomposition does provide an explicit relation for the L^2 minimum configuration.

7. STATISTICALLY-STORED DISLOCATIONS IN F.C.C. CRYSTALS

Classically, statistically-stored dislocation density has been considered to be comprised of dislocation dipoles and planar dislocation loops. In the formalism used to find ρ_{GN} with the L^1 minimization, a total of 27 SSD density vectors were found: only 18 of these were common dislocation dipoles. In the analysis of the null space of the linear operator \mathbf{A} in equation (31), nine other SSD structures were found which are neither simple dislocation dipoles nor simple planar loops. These higher-order closed structures are mathematically represented by the space spanned by the last nine vectors of the matrix in Table 2. An infinite number of SSD structures can be created by different combinations of the 27 null vectors found, but to illustrate the properties of higher-order SSD structures, the simplest in terms of the fewest number of lines and highest symmetry have been found. The simplest structure consists of five dislocation line segments and is mathematically represented, in varying orientations, by the last eight null vectors in Table 2. Interpreting the densities as dislocation line lengths as before, the vectors can be graphically rep-

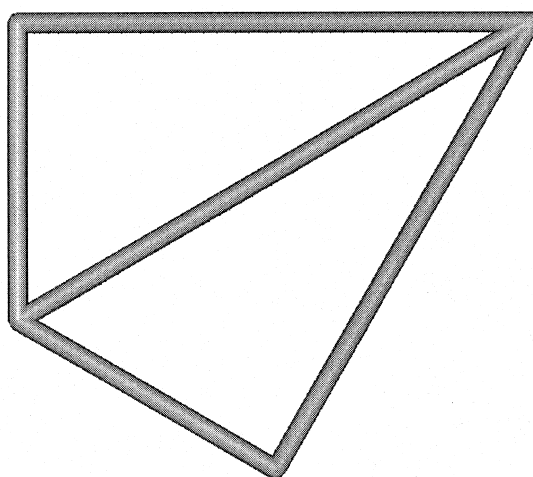


Fig. 10. A discrete planar dislocation structure representing the intersection of two dislocation loops with different Burgers vectors.

resented. The core structure corresponding to the last eight null vectors is shown in Fig. 10. The structure consists of a central edge dislocation which splits into two dislocations which loop around and connect back to the original center dislocation. The Burgers vectors of the three dislocation lines which compose this structure are different, and this structure could be created by the intersection of two expanding dislocation loops with different Burgers vectors on the slip plane. The result would be a dislocation arrangement like the one depicted. Note, however, that the two dislocations are not required to initially be on the same slip plane because, through cross-slipping, an intersection may also occur. These eight null vectors span the space of such dislocation interactions on all four slip planes.

The remaining SSD arrangement in Table 2 is made up of six edge dislocations in the three-dimensional structure shown in Fig. 11. Three of the dislocations are on the same slip plane with the other three lying, respectively, in the other three slip planes of the f.c.c. crystal lattice. This structure is

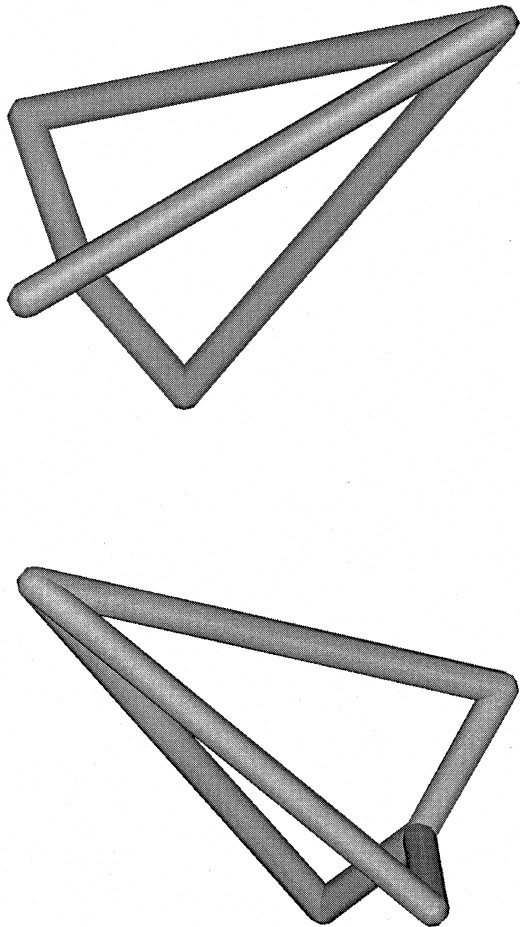


Fig. 11. A three-dimensional dislocation structure composed of six edge dislocations which self terminates and has no geometric consequence.

unique in that it contains a three-dimensional stacking fault whose boundaries are the edge dislocations shown in the figure. Since the extra half planes of atoms are fully contained within the structure, there is no geometric consequence over the volume containing the structure. Linear combinations of this vector with the other eight can create other, more complicated, three-dimensional SSDs. Figure 12 depicts a three-dimensional structure consisting of four screw dislocations on the perimeter of the structure and four edge dislocations in the interior of the structure, but as these three-dimensional structures become more complicated, it becomes harder to imagine their occurrence in real crystals.

In general, the higher-order dislocation structures in f.c.c. crystals primarily consist of dislocation loop segments which terminate at planar junctions. The total structure self-terminates, which is to say that the Burgers vector is conserved at each junction in the structure. The closed structures do not thread through the volume as do the crystallographic GNDs; furthermore, they do not create any dislocations which pierce the surface of the reference volume.

A general dislocation state for f.c.c. crystals in this basis of 36 linearly independent density vectors (nine crystallographic GND vectors, 18 dislocation dipole vectors, and nine higher-order SSD vectors) can be constructed by any linear combination of the 27 SSD vectors and the particular combination of GND vectors dictated by the value of Nye's tensor. This geometrically-allowable dislocation (GAD) density would conform to the geometric constraints, but would not restrict the total crystallographic dislocation density to any minimum principle. These vectors span the space of all glissile dislocations in f.c.c. crystals and could be used as a discrete dislocation basis for observed dislocation arrangements. Also, there may be other crystalline kinetic constraints which may suppress the population of dislocations on certain planes. The GAD density vector could be further restricted to reflect other such constraints.

8. GEOMETRICALLY-NECESSARY DISLOCATIONS IN POLYCRYSTALLINE AGGREGATES

In this article, parallels have been suggested between the determination of active slip systems from the plastic deformation tensor and the determination of crystallographic GNDs from Nye's tensor. In fact, the method used to determine ρ_{GN} using the L^1 minimization is analogous to the method employed by Taylor in the determination of the active slip systems in plastic deformation [14, 15]. Taylor's method was based on the principle of maximum work where the active slip systems were those which were specially oriented and required the least shearing to accomplish the desired deformation. The L^1 minimization of ρ_{GN} employs a

dicted by the use of Nye's tensor alone. Since the plastic resistance of a material is related to the square root of the dislocation density, the added resistance due to the presence of GNDs in these models is underestimated.

9. CONCLUDING REMARKS

This article has investigated the geometrical properties of GNDs and SSDs on a crystallographic dislocation basis. To describe crystallographic geometrically-necessary dislocations, a new formulation of Nye's dislocation tensor was introduced, based on the integrated properties of dislocation lines within a reference volume. A discretized version of the integral relation in which all crystallographic dislocations could be represented by a finite set of realizable crystallographic dislocation populations was adopted. The crystallographic GND state was found to be underdetermined by the constraints of Nye's tensor in crystals with a high degree of symmetry. This redundancy was overcome by employing minimum principles on two different density normalizations. The analyses were performed on an f.c.c. crystal lattice in which the dislocation populations were limited to either pure edge or pure screw type, and two categories of dislocation arrangements were found and visualized by considering dislocation density as a line length in a volume. The first category described crystallographic GNDs through periodic networks which maintained the same geometric properties and symmetries of the material GNDs they represented, and the second category described SSDs that were higher-order self-terminating dislocation structures which had no geometric consequence. From these two different types of arrangements, geometrically-allowable dislocation densities could be formulated which conformed to the geometric constraints of Nye's tensor. The implications of the crystallographic GND arrangements in single crystals on the presence of GNDs in polycrystalline materials due

to macroscopic plastic strain gradients culminated in the introduction of a Nye factor to account for underlying crystalline anisotropy.

Acknowledgements—We would like to thank the NSF under Grant No. 9700358 and the DoD through the NDSEG Fellowship Program for support of this research. We would also like to thank Ali S. Argon for his many discussions on the subject.

REFERENCES

1. Fleck, N. A., Muller, G. M., Ashby, M. F. and Hutchinson, J. W., *Acta metall. mater.*, 1994, **42**, 475.
2. Stölken, J. S. and Evans, A. G., *Acta mater.*, 1998, **46**, 5109.
3. Stelmashenko, N. A., Walls, M. G., Brown, L. M. and Milman, Y. V., *Acta metall. mater.*, 1993, **41**, 2855.
4. Ma, Q. and Clarke, D. R., *J. Mater. Res.*, 1995, **10**, 853.
5. Fleck, N. A. and Hutchinson, J. W., *J. Mech. Phys. Solids*, 1993, **41**, 1825.
6. Nix, W. D. and Gao, H., *J. Mech. Phys. Solids*, 1998, **46**, 411.
7. Nye, J. F., *Acta metall.*, 1953, **1**, 153.
8. Ashby, M. F., *Phil. Mag.*, 1970, **21**, 399.
9. Kröner, E., *Appl. Mech. Rev.*, 1962, **15**, 599.
10. Fleck, N. A. and Hutchinson, J. W., *Adv. appl. Mech.*, 1997, **33**, 295.
11. Gao, H., Huang, Y., Nix, W. D. and Hutchinson, J. W., Mechanism-based strain gradient plasticity—I. Theory, to be published.
12. Basinski, S. J. and Basinski, Z., in *Dislocations in Solids*, ed. F. R. N. Nabarro. North-Holland, Amsterdam, 1979.
13. Kubin, L. P., Canova, G., Condat, M., Devincre, B., Pontikis, V. and Brechet, Y., *Solid St. Phenomena*, 1992, **23/24**, 455.
14. Taylor, G. I., *Proc. R. Soc. Lond.*, 1934, **A145**, 362.
15. Taylor, G. I., *J. Inst. Metals*, 1938, **62**, 307.
16. Bishop, J. F. W. and Hill, R., *Phil. Mag.*, 1951, **42**, 414.
17. Bishop, J. F. W. and Hill, R., *Phil. Mag.*, 1951, **42**, 1298.
18. Dai, H. and Parks, D. M., Geometrically-necessary dislocation density in continuum crystal plasticity theory and FEM implementation, to be published.